

# Differential Chromatic Refraction: literature overview

I. S. Sullivan, D. J. Reiss

November 16, 2015

## 1 Overview

Like any medium, the Earth's atmosphere refracts incident light, which for an observer on the Earth's surface results in a deflection of the apparent position of sources towards zenith by about 1 arcsecond per degree of the source from zenith. This bulk effect of refraction is well understood in astronomical applications and is easily accounted for most of the optical through radio wavelengths where the index of refraction is constant, but towards the blue end of the optical spectrum atmospheric dispersion results in increasing refraction. As a result, photons from the same source but different wavelengths that pass through the same filter of a telescope will have slightly different degrees of refraction and will land on different locations of the detector, an effect called Differential Chromatic Refraction (DCR). Differential Chromatic Refraction was first raised as an issue for spectrometry in Filippenko (1982), where the problem was framed as a loss of flux in slit spectrometers. The issue has now become important for imaging cameras as well, though, because high-resolution cameras such as the LSST will experience significant PSF smearing in the *u* and *g* bands (Figure 1).

## 2 DCR literature

A quick summary of and notes on the existing literature covering DCR. Each reference we found is covered in it's own subsection below.

### 2.1 Report on Summer 2014 Production: Analysis of DCR (Andrew Becker)

[https://github.com/lsst-dm/S14DCR/blob/master/report/S14report\\_V0-00.pdf](https://github.com/lsst-dm/S14DCR/blob/master/report/S14report_V0-00.pdf)

- Estimated DCR effects directly for LSST using catSim's stellar SEDs.
- Investigated only airmass effects (no temperature, etc. dependence).
- Utilized 5 mas threshold for "good" DCR corrections based on estimated accuracy required for difference imaging (no dipoles).
- Summary of DCR estimates:
  - For *g* and *r*, nearly all stars will exhibit differential DCR of  $> 5$  mas at parallactic angle differences  $> 20$  deg. or airmass differences of  $> 0.15$ .
  - For *i*, similar effects for parallactic angle differences  $> 25$  deg. or airmass differences  $> 0.2$ , mostly for M-dwarf stars.
  - For *z*, only very large differences in parallactic angle or airmass lead to DCR  $> 5$  mas.
- DCR corrections tested based on modeling using colors and airmass terms.
  - Random forest regression models provided most accurate modeling of DCR and refraction.
  - *u* and *g* models worked but would be degraded by 10% color errors (*u*) or 2.5% color errors (*g*).
  - *riz* models could correct all but  $10^{-5}$  stars to  $< 5$  mas residuals.

**\*\*Recommendations\*\*:**

- Code from the S14DCR analysis <https://github.com/lsst-dm/S14DCR> should be updated to use latest version of sims\_photUtils and include estimates for galaxies and SNe.
- Understand how DCR calcs are performed in sims pipeline to compare the results of these simulations to DCR effects in simulated images, and to enable investigation of DCR corrections on image coadds and differences (see also <https://github.com/lsst-dm/W14ImageDifferencing>).

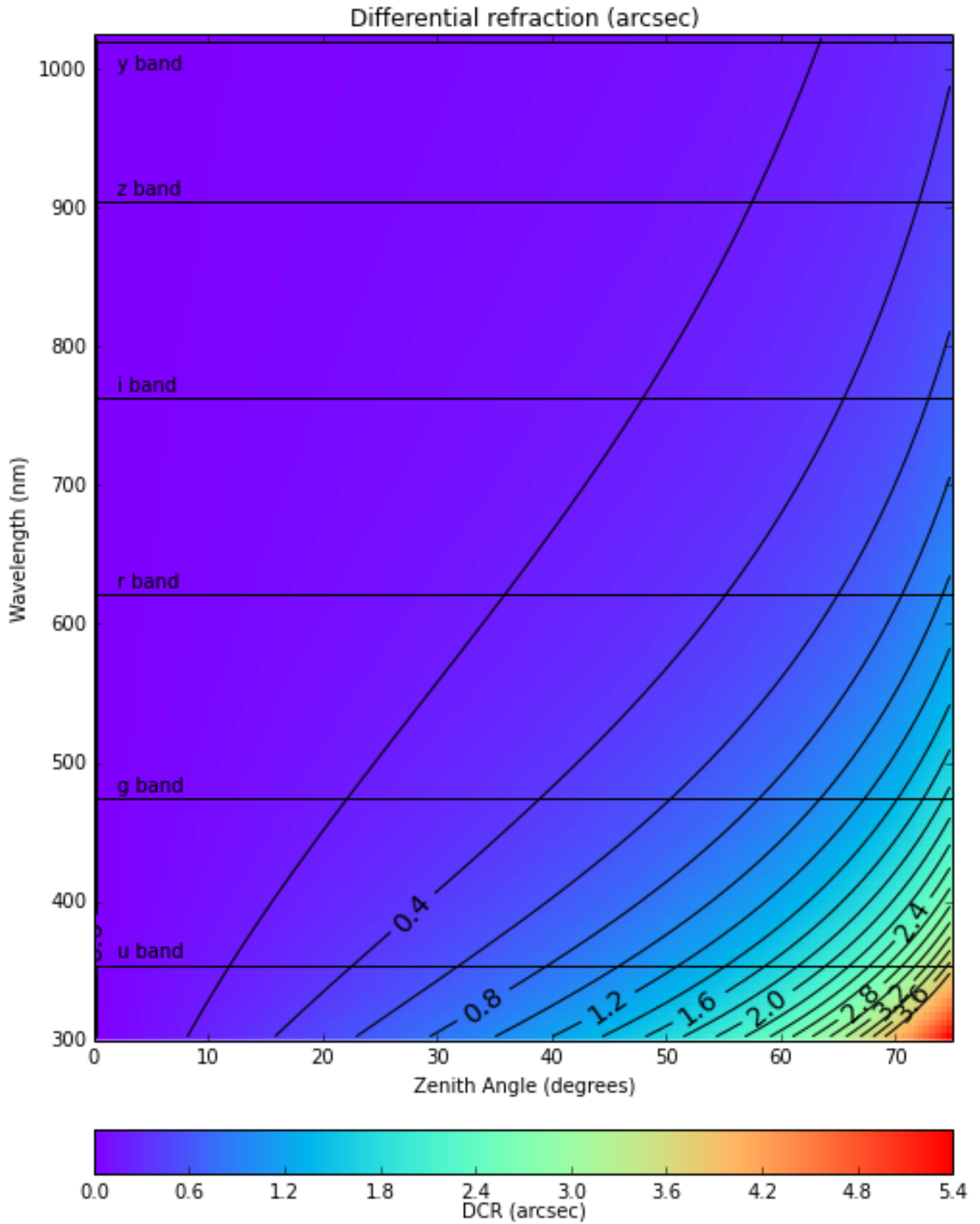


Figure 1: Maximum DCR over a range of zenith angles and wavelengths. Each wavelength is treated as the center wavelength of a band with 20% bandwidth, and maximum DCR is calculated for the difference in position of two photons from the same source at opposite ends of the band.

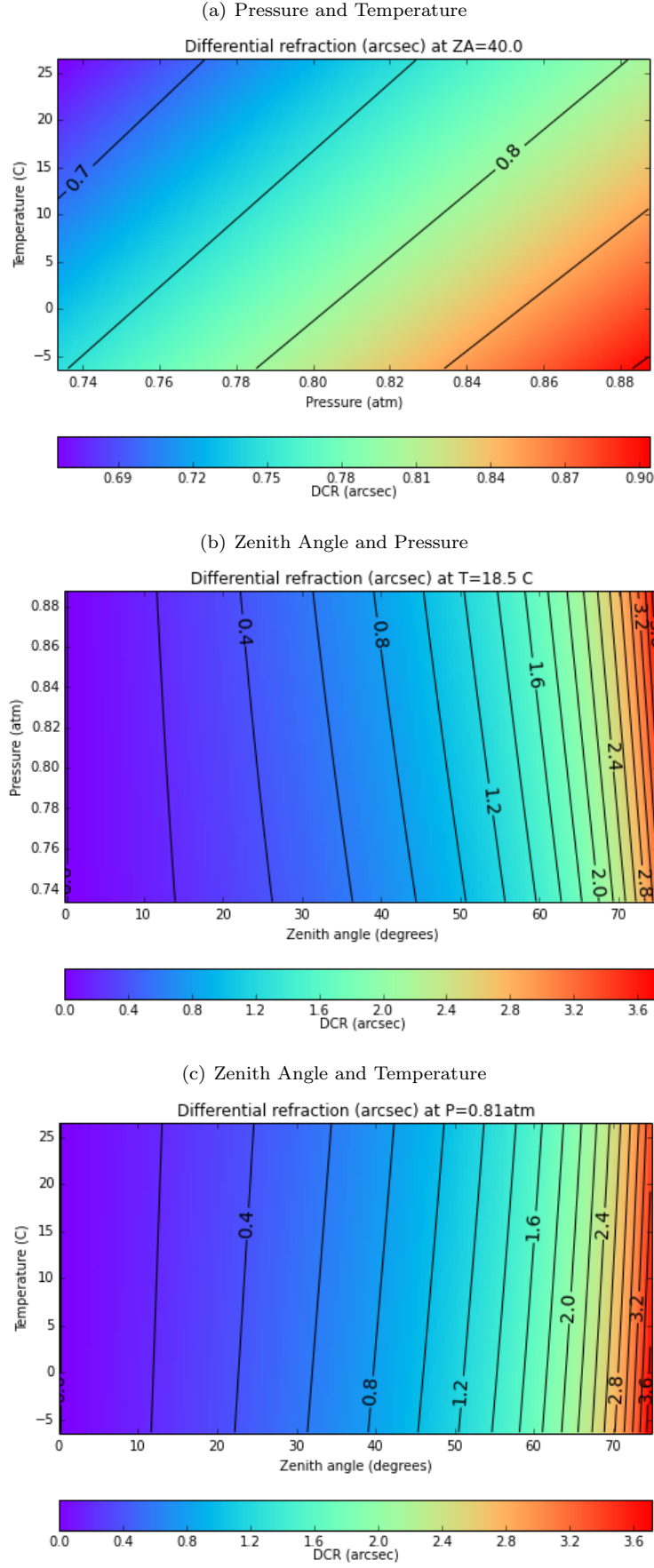


Figure 2: Investigation of maximum DCR under varying conditions for LSST  $u'$  band. For a given filter, maximum DCR depends on the zenith angle of observation (airmass), atmospheric pressure, temperature, and, to a lesser degree, humidity. In panels (a) - (c) we keep one of the three main parameters fixed at a nominal value, and map the full range of realistic observing conditions for the remaining two to get a feel for the relative importance of each.

## 2.2 Meyers and Burchat (2015)

- Estimates of DCR on weak lensing measurements.
- Source code for analysis is available here: <https://github.com/DarkEnergyScienceCollaboration/chroma/>.
- Primarily measured effects of DCR on shape measurements (2nd moments); code can be used to estimate 1st moments for a given SED. Preliminary code: <https://github.com/isullivan/LSST-DCR/tree/master/code/notebooks>.
- Also investigated effects of 1st moments for galaxy SEDs and compensation via extra trees regression on LSST colors.

## 2.3 Chambers (2005)

- Updated summary of (more accurate?) astrometric transformations including DCR.
- Estimated astrometric accuracy in Pann-STARRS of 1 mas. This assumes accurate atmospheric characterization for each field from sky probes (atmospheric absorption).

**\*\*Recommendations\*\*:**

- Understand these transformations. Suggestion is that C code exists somewhere in the Pan-STARRS codebase, but I could not find it.

## 2.4 Cuby et al. (1998)

## 2.5 Filippenko (1982)

- Original paper posing DCR as a problem to be addressed.
- Focused on the effect on spectrometers, with the recommendation that slit spectrometers be aligned with fixed parallactic angle.

## 2.6 Alcock et al. (1999)

- Investigation of DiffIm for MaCHO search.
- This is the only reference I could find that described a method to correct for DCR for image differencing. Suggestion is to compute a per-pixel color map of each field (using images near zenith or at least at the same airmass and parallactic angle). They then interpolated the pixel values in the template image based on the color map pixel values, the airmass of the observation relative to the reference image, and the parallactic angle of the observation.
- Improvements were obtained by differencing a number of images taken at a range of airmasses to obtain a semi-empirical result for the offset required with color and airmass (relative to the reference image).
- The results shown in Figure 5 suggest moderate success with this strategy.

## 2.7 Alejandro Plazas and Bernstein (2012)

## 2.8 Stone (1996)

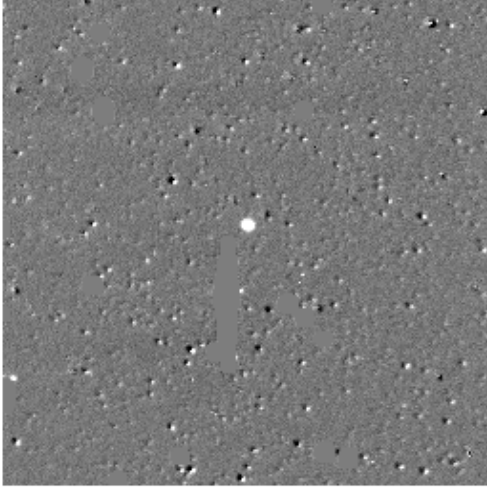
- A good reference giving equations for refraction including the effect of temperature, pressure, and water vapor pressure. Used for calculating Figure 2

The refraction of monochromatic light is given by

$$\begin{aligned} R(\lambda) &= r_0 n_0(\lambda) \sin z_0 \int_1^{n_0(\lambda)} \frac{dn}{n (r^2 n^2 - r_0^2 n_0(\lambda)^2 \sin^2 z_0)^{1/2}} \\ &\simeq \kappa(n_0(\lambda) - 1)(1 - \beta) \tan z_0 - \kappa(1 - n_0(\lambda)) \left( \beta - \frac{n_0(\lambda) - 1}{2} \right) \tan^3 z_0 \end{aligned} \quad (1)$$

where  $n_0(\lambda)$ ,  $\kappa$ , and  $\beta$  are given by equations 2, 3, and 4 below, respectively.

(a) Difference image with no DCR correction



(b) Difference image with DCR correction

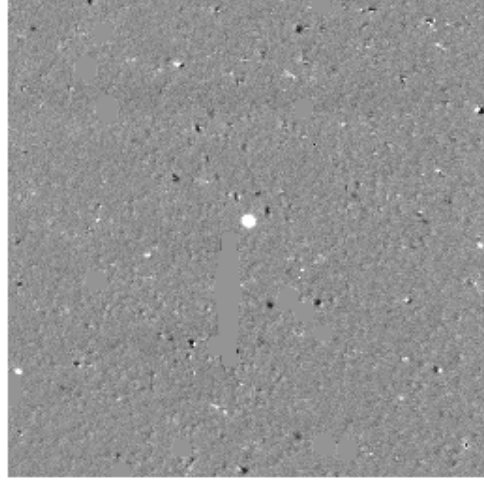


Figure 3: (Alcock et al. Fig. 5.) "The effect of differential refraction on difference images. Left image is a difference image without applying any correction for differential refraction effects. The right image is the same image with our correction technique applied. The scale of the noise structures is much reduced although not completely removed. The two images are 100 100. The residual object in the centre is due to a variable star"

Parameter	valid range	description	units
$P_s$	$0 \text{ mbar} < P_s < 4000 \text{ mbar}$	Atmospheric pressure	millibar
$RH$	$0\% < RH < 100\%$	Relative humidity	Percent
$\lambda$	$2302\text{\AA} < \lambda < 20,586\text{\AA}$	Wavelength	Angstroms
$T$	$250K < T < 320K$	Temperature	Kelvin
$\phi$	$0^\circ \leq \phi < 360^\circ$	Latitude of the observing site	Degrees
$h$	$0 \text{ m} \leq h$	Elevation of the observing site	meters
$z_0$	$0^\circ \leq z_0 < 75^\circ$	Zenith angle	Degrees

Table 1: Definition of parameters and their units

To calculate refraction, we need to know the local index of refraction of air  $n_0(\lambda)$  at the observatory site:

$$n_0(\lambda) = 1 + \left( \left[ 2371.34 + \frac{683939.7}{130 - \sigma(\lambda)} + \frac{4547.3}{38.9 - \sigma(\lambda)^2} \right] D_s + (6487.31 + 58.058\sigma(\lambda)^2 - 0.71150\sigma(\lambda)^4 + 0.08851\sigma(\lambda)^6) D_w \right) \times 10^{-8} \quad (2)$$

where

$$\sigma(\lambda) = 10^4 / \lambda \quad (\mu\text{m}^{-1})$$

$$D_s = \left[ 1 + (P_s - P_w) \left( 57.90 \times 10^{-8} - \frac{9.3250 \times 10^{-4}}{T} + \frac{0.25844}{T^2} \right) \right] \frac{(P_s - P_w)}{T}$$

$$D_w = \left[ 1 + P_w (1 + 3.7 \times 10^{-4} P_w) \left( -2.37321 \times 10^{-3} + \frac{2.23366}{T} - \frac{710.792}{T^2} + \frac{7.75141 \times 10^4}{T^3} \right) \right] \frac{P_w}{T}$$

$$P_w = RH \times 10^{-4} \times e^{(77.3450 + 0.0057T - 7235.0/T)/T^{8.2}}$$

The ratio of local gravity at the observing site to  $g = 9.81 \text{ m/s}^2$  is given by

$$\kappa = g_0/g = 1 + 5.302 \times 10^{-3} \sin^2 \phi - 5.83 \times 10^{-6} \sin^2(2\phi) - 3.15 \times 10^{-7} h \quad (3)$$

If we assume an exponential density profile for the atmosphere, then the ratio  $\beta$  of the scale height of the atmosphere to

radius of the observing site from the Earth's core can be approximated by:

$$\begin{aligned}\beta &= \frac{1}{R_{\oplus}} \int_0^{\infty} \frac{\rho}{\rho_0} dh \\ &\simeq \frac{P_s}{\rho_0 g_0 R_{\oplus}} = \frac{k_B T}{m g_0 R_{\oplus}} \\ &= 4.5908 \times 10^{-6} T\end{aligned}\tag{4}$$

where  $m$  is the average mass of molecules in the atmosphere,  $R_{\oplus}$  is the radius of the Earth,  $k_B$  is the Boltzmann constant, and  $g_0$  is the acceleration due to gravity at the Earth's surface.

## References

- Alcock, C., Allsman, R. A., Alves, D., Axelrod, T. S., Becker, A. C., Bennett, D. P., Cook, K. H., Drake, A. J., Freeman, K. C., Griest, K., Lehner, M. J., Marshall, S. L., Minniti, D., Peterson, B. A., Pratt, M. R., Quinn, P. J., Stubbs, C. W., Sutherland, W., Tomaney, A., Vandehei, T., Welch, D. L., and Collaboration, M. (1999). Difference image analysis of galactic microlensing. I. Data analysis. *Astrophysical Journal*, 521(2, 1):602–612.
- Alejandro Plazas, A. and Bernstein, G. (2012). Atmospheric Dispersion Effects in Weak Lensing Measurements. *Publications of the Astronomical Society of the Pacific*, 124(920):1113–1123.
- Chambers, K. C. (2005). Astrometry with Pan-STARRS and PS1: Pushing the limits of atmospheric refraction, dispersion, and extinction corrections for wide field imaging. *Astrometry in the Age of the Next Generation of Large Telescopes*, 338(Vieira 2005):134–144.
- Cuby, J. G., Bottini, D., and Picat, J. P. (1998). Handling atmospheric dispersion and differential refraction effects in large-field multiobject spectroscopic observations. In D'Odorico, S., editor, *Proc. SPIE Vol. 3355*, volume 3355, pages 36–47.
- Filippenko, A. V. (1982). The importance of atmospheric differential refraction in spectrophotometry. *Publications of the Astronomical Society of the Pacific*, 94(August):715.
- Meyers, J. E. and Burchat, P. R. (2015). IMPACT OF ATMOSPHERIC CHROMATIC EFFECTS ON WEAK LENSING MEASUREMENTS. *The Astrophysical Journal*, 807(2):182.
- Stone, R. C. (1996). An Accurate Method for Computing Atmospheric Refraction. *Publications of the Astronomical Society of the Pacific*, 108(729):1051.